VIP Intermetallic Phases

DOI: 10.1002/ange.201207076

A Sodium-Containing Quasicrystal: Using Gold To Enhance Sodium's Covalency in Intermetallic Compounds**

*Volodymyr Smetana, Qisheng Lin, Daniel K. Pratt, Andreas Kreyssig, Mehmet Ramazanoglu, John D. Corbett, Alan I. Goldman, and Gordon J. Miller**

Quasicrystals (QCs) exhibit crystallographically forbidden rotational symmetries and aperiodic long-range positional order.[1] Three-dimensional quasicrystals, that is, icosahedral quasicrystals (*i*-QCs) belong to one of three commonly accepted subtypes: 1) Bergman; 2) Mackay; and 3) Tsai types,[2] which are differentiated by their atom clusters that are also essential structural components of corresponding crystalline approximants. Approximants are periodic crystals with similar chemical compositions to nearby QCs. After the discovery of the first *i*-QC in rapidly quenched Al–Mn,[3] many stable and metastable species have been synthesized with elements that span major portions of the periodic table (Figure 1 a). None of these *i*-QCs nor any other QC, however, contain Na, although numerous Na-containing Bergman-type structures, such as $Na_{16}Mg_{36}Al_{40}Zn_{68}$,[4] $Na_{13}Cd_{20}Pb_7$,[5] $Na_{13}Cd_{18.9}Tl_{8.1}$,[6] $Na_{26}Au_{40.9}Ge_{14.1}$, and $Na_{26}Au_{39.8}Sn_{15.2}$,[7] have been reported. Herein, we report the discovery and characterizations of the first Na-containing *i*-QC, *i*-$Na_{13}Au_{12}Ga_{15}$, which belongs to the Bergman type but has an extremely low valence electron-to-atom (*e*/*a*) value of 1.75 for such phases (Figure 1 b). By analyzing the electronic structure of the 1/1 approximant structure, the existence and stability of this Na-containing *i*-QC is tightly linked to its substantial Au content, which allows the *e*/*a* value to satisfy a Hume–Rothery stabilization rule and creates novel Na–Au polar-covalent interactions.

This new *i*-QC was discovered during systematic exploration of the Na–Au–Ga system to uncover novel polar intermetallics with complex Au–Ga frameworks. Phases that were identified in the narrow region near 32 at % Na with Au/Ga molar ratios ranging from approximately 1:2 to 2:1 (see Figure 2) include a stuffed (Ga-centered) Bergman 1/1 phase,

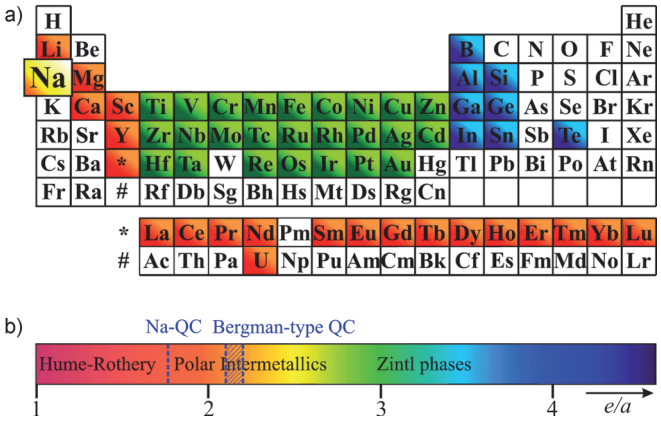

Figure 1. a) The elements in the periodic table that are reported to form quasicrystalline compounds are colored. All of the known quasicrystals contain representatives from at least two of the three different classes of elements (coded by orange, green, and blue). b) Positions of Bergman-type quasicrystals and the present Na-containing quasicrystal in terms of the valence electron count per atom (*e*/*a*) values.

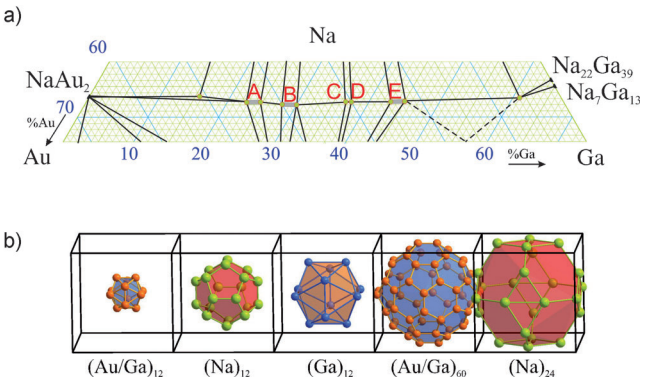

Figure 2. a) The 350 °C isothermal segment of the Na–Au–Ga diagram in the range of 25–40 atomic percent of Na. **A** = $Na_{26}Au_{36}Ga_{19}$, **B** = $Na_{32}Au_{38}Ga_{30}$, **C** = $Na_{26}Au_{25}Ga_{29}$, **D** = *i*-$Na_{13}Au_{12}Ga_{15}$, **E** = $Na_{26}Au_{18}Ga_{36}$. The atomic percentages of Au and Ga, and the binaries $NaAu_2$, Na_7Ga_{13}, and $Na_{22}Ga_{39}$ are marked. b) Concentric clusters in the structure of **E** that lie at the center.

$Na_{26}Au_{36}Ga_{19}$ (**A**),[7] an orthorhombic approximant $Na_{32}Au_{38}Ga_{30}$ (**B**), a 2/1 approximant $Na_{26}Au_{25}Ga_{29}$ (**C**), an *i*-QC phase *i*-$Na_{13}Au_{12}Ga_{15}$ (**D**), and a conventional (uncentered) Bergman 1/1 phase $Na_{26}Au_{18}Ga_{36}$ (**E**).[7] **A**, **B**, and **E** have recognizable phase widths. The new *i*-QC (**D**), which is obtained reproducibly from sample loadings indicated in

[*] Dr. V. Smetana, Dr. Q. Lin, Prof. J. D. Corbett, Prof. G. J. Miller
Department of Chemistry, Ames Laboratory, US-DOE
Iowa State University, Ames, IA 50011 (USA)
E-mail: gmiller@iastate.edu
Dr. D. K. Pratt, Dr. A. Kreyssig, Dr. M. Ramazanoglu, Prof. A. I. Goldman
Department of Physics and Astronomy, Ames Laboratory
US-DOE, Iowa State University, Ames, IA 50011 (USA)

[**] We are indebted to J. Jacobs for ICP-MS analyses and K. Dennis for DSC measurements. The research was supported by the Office of the Basic Energy Sciences, Materials Sciences Division, U. S. Department of Energy (DOE). Ames Laboratory is operated for DOE by Iowa State University under contract No. DE-AC02-07CH11358. Use of the Advanced Photon Source was supported by the US DOE under Contract No. DE-AC02-06CH11357.

Supporting information for this article is available on the WWW under http://dx.doi.org/10.1002/anie.201207076.

Table S1 in the Supporting Information, displayed a simple X-ray powder diffraction pattern that could not be indexed by using a conventional crystallographic unit cell (Figure 3a),

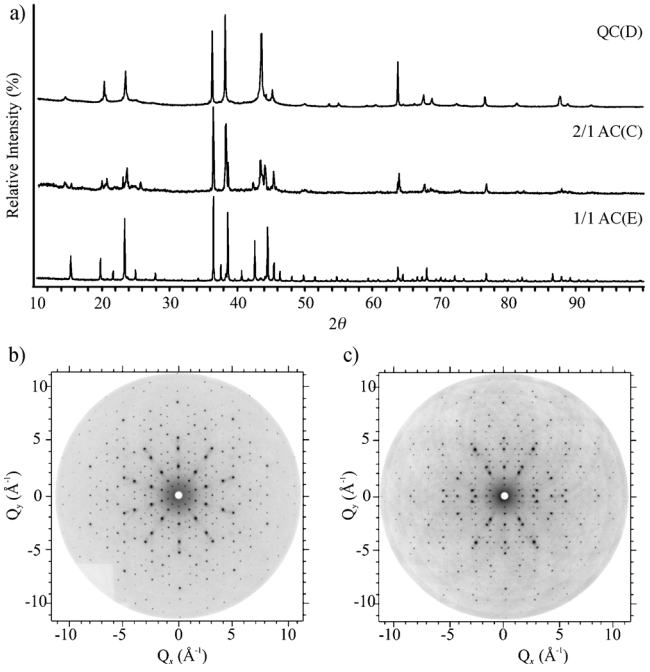

Figure 3. a) X-ray powder diffraction patterns of the quasicrystal (**D**), the 2/1 (**C**), and the 1/1 approximants (**E**). The zero-level high-energy precession images of the single-grain quasicrystal viewed along b) the fivefold and c) the twofold axes.

but it was semiquantitatively recognized as arising from a probable Bergman-type quasicrystalline structure, based on experience with Ca–Au–Ga/In/Sn systems.[8] Furthermore, this pattern is similar to those of the 1/1 and 2/1 Bergman-type approximants, patterns of which are also included in Figure 3a.

A thorough single-grain investigation was carried out using a high-energy X-ray precession camera at the advanced photon source (see the Supporting Information for details). Figures 3b and c display the zero-level precession images along the fivefold and twofold axes of the sample for an incident X-ray wavelength of 0.125 Å ($E = 100$ keV). All diffraction spots in these images can be indexed to a primitive icosahedral quasilattice,[9] with group $Pm\bar{3}\bar{5}$ and a quasilattice constant of $a_R = 5.264(4)$ Å, a value that represents the largest reported quasilattice constant among Bergman-type *i*-QCs.[2] There is, however, some evidence of diffuse streaks in the twofold plane that are oriented parallel to the threefold axes of the sample. These streaks generally indicate the presence of some degree of residual phason strain in the sample that originates from defects in tiling arrangements of the icosahedral structure[10] (see the Supporting Information).

Although the exact atomic structure of *i*-QC remains unknown, insights arise by examining the first-ever occurrence of both conventional (**E**) and stuffed (**A**) Bergman-type 1/1 potential approximants.[7] The structure of **E** consists of a central $(Au/Ga)_{12}$ icosahedron surrounded, in successive shells, by a dodecahedron of 20 Na atoms, a larger icosahedron of 12 Ga atoms, a truncated icosahedron of a 60-atom Au/Ga mixture, and a defect triacontahedron of 24 Na atoms (see Figure 2b). In the case **A**, which contains a higher proportion of Au atoms, certain positions that are mixed Au/Ga in **E** are fully occupied by Au atoms and, more significantly, the inner icosahedron is centered by an additional Ga atom.[7] However, **E** should be the appropriate 1/1 approximant because its lattice parameter (14.512(2) Å) is within three standard deviations from that calculated (14.490(11) Å) from the quasilattice constant of *i*-QC by using the equation $a_{q/p} = 2a_R(p + q\tau)/(2 + \tau)^{1/2}$,[11] where q/p denotes the order of the approximant, and τ is the golden mean ($\tau = (\sqrt{5} + 1)/2$), $a_R = 5.264(4)$ Å. In comparison, the lattice parameter for the stuffed Bergman phase **A** (14.597(2) Å) is much larger. In fact, **E** is also closer to **D** in chemical composition (see Figure 2a).

The differential scanning calorimetry (DSC) data of *i*-$Na_{13}Au_{12}Ga_{15}$ showed reversible endothermic and exothermic events on heating and on cooling, respectively, at 551.3 °C and 536.4 °C (Figure 4); these events are a signature of a stable

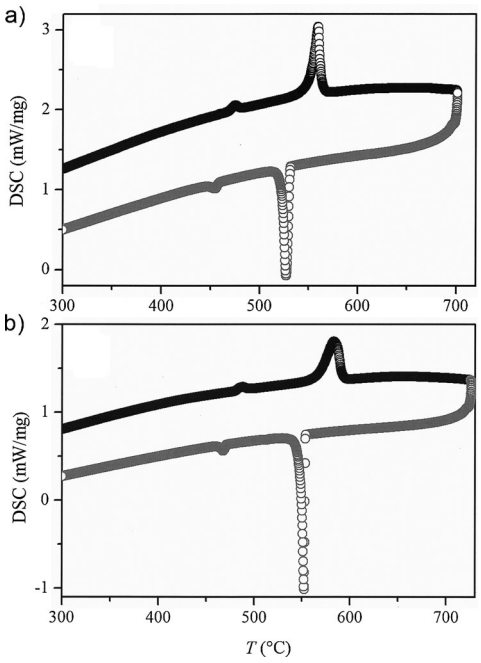

Figure 4. The DSC data (on heating: black, upper curves; on cooling: gray, lower curves) of a) the quasicrystal $Na_{13}Au_{12}Ga_{15}$ (**D**) and b) the orthorhombic phase $Na_{32}Au_{38}Ga_{30}$ (**B**).

phase with probable congruent melting and crystallization processes. Similar events occur for crystalline phase **B**, but at 567.0 °C and 553.2 °C. However, both **B** and **D** also showed minor events at approximately 470 °C and 474 °C; these events possibly arise from the 2/1 approximant phase (**C**). Although **C** was not readily detected by powder X-ray diffraction of **B** or **D**, its presence is possible because of uncertainties in sample compositions.

This new Na–Au–Ga QC is notable for two reasons. First, although Bergman-type *i*-QCs may contain the electropos-

itive metals Li and Mg, this Na-based system is the first to feature any of the heavier alkali metals. The absence of Na-containing QCs has been rationalized by Na's small absolute electronegativity (2.85), as compared to those of Li (3.01) and Mg (3.75);[12] this small absolute electronegativity suggests that Na lacks sufficient covalency to stabilize Bergman-type *i*-QCs. In contrast, Li and Mg can act as either a formal electron donor or an electron acceptor. Secondly, the *e*/*a* value for *i*-$Na_{13}Au_{12}Ga_{15}$ is exceptionally low, that is, 1.75 (without counting the $5d^{10}$ electrons of Au), which is far below the favorable range for traditional Bergman-type phases (2.1–2.2). For example, *i*-Li_3CuAl_6[13] and *i*-Li_3AuAl_6[14] are known Bergman-type QCs that contain elements from the same chemical groups as those in $Na_{13}Au_{12}Ga_{15}$, yet their *e*/*a* values are 2.20, owing to the low Cu or Au content and large percentage of Al. In fact, the *e*/*a* value alone cannot unequivocally distinguish different types of Hume–Rothery phases, including QCs, particularly among those cases for which the Fermi surfaces are mediated by transition metal d orbitals, such as Tsai-type *i*-QCs and approximants in the Ca–Au–In/Ga/Sn systems.[8] Rather, the stability of a Hume–Rothery phase arises from the interactions between the Fermi surface, which is set by the *e*/*a* value, and a Jones zone formed by critical reciprocal lattice vectors, G, where $|G| = \sqrt{h^2+k^2+l^2}$ in units of $2\pi/a$ ($2\pi/a$; a = real space lattice vector).[15] Actually, we have confirmed[7] that the formation of a pseudogap for $Na_{13}Au_{12}Ga_{15}$ ($e/a = 1.75$), a hypothetical 1:1 approximant model with the same composition as *i*-QC, is the result of Fermi surface—Brillouin zone interactions, in accord with Mizutani's analysis.

The combination of Au with Na and Ga in the QC and its approximants contribute to the thermodynamic stability of the QC with respect to decomposition by establishing polar-covalent Au–Ga and even Au–Na metal–metal bonds. The remarkably large variety of new and unusual structures[16] arising from recent investigations of numerous ternary A–Au–M systems (A = alkali or alkaline-earth metals; M = Zn, Cd, Ga, In, Tl, Si, Ge, Sn, and Te) attests to the aforementioned conclusion. Accompanying theoretical studies point to the significance of Au–M polar-covalent bonding in these systems, such that these interactions often comprise 65–90% of the total crystal orbital Hamilton population (COHP), which is a semi-quantitative measure of covalent-bonding contributions in solids. Although Na binding in a crystalline Bergman phase is not unusual,[4–7] its participation in delocalized metal–metal bonding, an important feature of a QC, is unexpected. Clear evidence for significant Na involvement in bonding in *i*-$Na_{13}Au_{12}Ga_{15}$ can be extracted from the density of state (DOS) curves and COHP analyses of Na–Au–Ga approximants, as well as the Na–Au distances. Figure 5 shows the DOS and COHP data for $Na_{13}Au_{12}Ga_{15}$, a model built with the structural parameters of **E** and the composition of the *i*-QC **D**. The Fermi level (E_F) lies near a sharp pseudogap, which corresponds to optimized Au–Ga and Ga–Ga orbital interactions. Of particular importance, however, is the comparison of the Na–Au and Na–Ga COHP curves, which represent the most polar interactions but their covalent bonding contributions are greatly enhanced by the substantial Au content. Analysis of the total COHP reveals

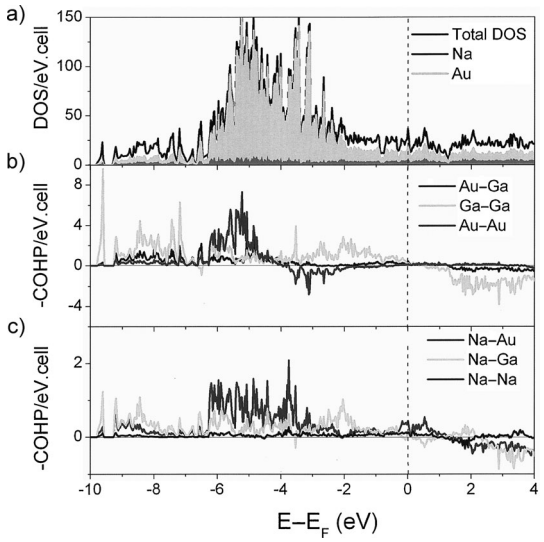

Figure 5. The DOS and COHP curves for "$Na_{26}Au_{24}Ga_{30}$" in a 1/1 Bergman-type approximant structure. The Fermi level (0 eV) for the calculated composition is marked by the dashed line. Positive −COHP values are bonding states; negative −COHP values are antibonding states. a) DOS curve with contributions from Au (light gray) and Na (dark gray) are highlighted. Au 5 d and 6 s and Ga 4 s and 4 p orbitals make the principal contributions to all occupied states. b) COHP curves for Au–Ga (black), Ga–Ga (light gray), and Au–Au (dark gray). c) COHP curves for Na–Au (dark gray), Na–Ga (light gray), and Na–Na (black). Note the different scales for the two sets of COHP curves.

that Au–Au and Au–Ga interactions constitute 14.7% and 37.0%, respectively, of the total bonding population, whereas Na–Au and Na–Ga contribute 9.3% and 8.6%, respectively. The contribution of the Na–Au bonding population is especially surprising and not at all in accord with classical expectations of marginal sodium covalency in such phases. These values are comparable with the approximately 16% contribution from Li–Au and Li–Al in "$Li_{26}Au_{12}Al_{42}$", an approximant model of *i*-Li_3AuAl_6 (see the Supporting Information, Table S2). In contrast, the total Na–Au and Na–Ga contributions for the stuffed Bergman-type (**A**) is considerably smaller, approximately 12% (see the Supporting Information, Table S2). An experimental, albeit qualitative, indicator for strong Na–Au bonding also arises from unusually small Na–Au distances, that is, 3.06–3.15 Å,[17] observed in many Bergman-type crystalline phases and related structures. Evidence of the typically stronger covalent bonding between alkaline-earth metals and gold have been noted before.[8a,18]

The discovery of the first Na-containing *i*-QC, $Na_{13}Au_{12}Ga_{15}$, should stimulate renewed interest for new elements that can be incorporated into quasicrystals. Are there more Na-containing QCs? Are there quasicrystals containing more-active metals (such as K or Sr) with less covalent character? Although the phrase "first comes the synthesis"[19] is always true, one lesson learned from the present study is that *i*-QCs likely emerge from ternary derivatives of existing binary alkali metal/post transition metal systems that already contain icosahedra. Compared with the binary phases in the Na–Ga, Na–Ge, and Na–Sn systems, it is known that rhombohedral Na_7Ga_{13} contains

Bergman-type building blocks,[20] some of which are modified to give 72 atom instead of 60 atom, buckyball-type, outer shells; in contrast, no binary structures in the Na–Ge and Na–Sn systems contain icosahedral clusters or fragments thereof. As a matter of fact, our investigations into related Na-containing ternary intermetallic mixtures in Na–Au–Ge and Na–Au–Sn have not yielded any QCs.[7] Following the same principle, it would be of interest to reexamine the Na–Au–In system, which includes not only several Na–In phases with local icosahedral symmetry,[21] but also the isostructural
Na–Au–In Bergman phases.

Experimental Section

Synthesis: Reaction mixtures, comprising of 300–500 mg of each of the pure metals (Na, 99.95%, Alfa-Aesar, surfaces manually cleaned with a surgical blade; Au, 99.999%, Ames Laboratory; Ga, 99.999%, Alfa-Aesar) were welded into Ta tubes under Ar, and then sealed into evacuated fused silica ampoules. These reaction mixtures were heated at 750°C for 3–5 h, cooled to 350°C at a rate of 4°C per hour, annealed for 3–5 days, and finally quenched in water. All products show a metallic luster and are stable in air at room temperature for months according to powder X-ray diffraction patterns. The sample composition for the quasicrystalline phase **D** was found to be $Na_{26}Au_{25(2)}Ga_{29(1)}$ by inductively coupled plasma-mass spectroscopy (ICP–MS).

Thermal analysis: Samples of **D** (42 mg) and **B** ($Na_{32}Au_{38}Ga_{30}$; 35 mg) were analyzed using a Netzsch DSC 404 C. Samples enclosed in Ta ampoules (ϕ 2 × 20 mm^3) under argon were heated to 720°C at a rate of 10°C min^{-1}, kept at this temperature for 15 min, and cooled to 100°C at the same rate. Additional DSC experiments on other samples conducted to 900°C yielded no other observable events.

X-ray diffraction: Powder X-ray diffraction data was collected using a Panalytical X′Pert Pro powder diffractometer equipped with Cu $K\alpha_1$ radiation ($\lambda = 1.540598$ Å). The diffraction peaks of the icosahedral quasicrystal can be indexed using 6D space according to the Elser's method.[22] A single grain quasicrystal from sample No. 4 (see the Supporting Information, Table S1) was selected for diffraction measurements by using a newly developed high-energy X-ray precession camera technique on station 6ID-D at the Advanced Photon Source.[23]

Received: August 31, 2012
Published online: November 28, 2012

Keywords: intermetallic phases · metal–metal interactions · quasicrystals

[1] C. Janot, *Quasicrystals: A Primer*, 2nd ed., Oxford University Press, Oxford, UK, **1994**.
[2] W. Steuer, S. Deloudi, *Crystallography of Quasicrystals*, Springer, Berlin, **2009**.
[3] D. Shechtman, I. Blech, D. Gratias, J. W. Cahn, *Phys. Rev. Lett.* **1984**, *53*, 1951 – 1953.
[4] M. Elding-Pontén, S. Lidin, *J. Solid State Chem.* **1995**, *115*, 270 – 273.
[5] E. Todorov, S. C. Sevov, *Inorg. Chem.* **1997**, *36*, 4298 – 4302.
[6] B. Li, J. D. Corbett, *Inorg. Chem.* **2004**, *43*, 3582 – 3587.
[7] Q. Lin, V. Smetana, G. J. Miller, J. D. Corbett, *Inorg. Chem.* **2012**, *51*, 8882 – 8889.
[8] a) Q. Lin, J. D. Corbett, *J. Am. Chem. Soc.* **2007**, *129*, 6789 – 6797; b) Q. Lin, J. D. Corbett, *Inorg. Chem.* **2008**, *47*, 7651 – 7659; c) Q. Lin, J. D. Corbett, *Inorg. Chem.* **2010**, *49*, 10436 – 10444.
[9] N. D. Mermin, *Rev. Mod. Phys.* **1992**, *64*, 3 – 49.
[10] P. A. Bancel in *Quasicrystals: The State of the Art* (Eds.: D. P. Divincenzo, P. J. Steinhart), World Scientific, Singapore, **1999**, pp. 17 – 54.
[11] A. I. Goldman, K. F. Kelton, *Rev. Mod. Phys.* **1993**, *65*, 213 – 230.
[12] R. G. Pearson, *Inorg. Chem.* **1988**, *27*, 734 – 740.
[13] P. Sainfort, B. Dubost, *J. Phys. (France)* **1986**, *47*, 321 – 330.
[14] H. S. Chen, J. C. Phillips, P. Villars, A. R. Kortan, A. Inoue, *Phys. Rev. B* **1987**, *35*, 9326 – 9329.
[15] U. Mizutani, *Hume-Rothery Rules for Structurally Complex Alloy Phases*, CRC, London, **2011**.
[16] J. D. Corbett, *Inorg. Chem.* **2010**, *49*, 13 – 28.
[17] S. L. Samal, Q. Lin, J. D. Corbett, *Inorg. Chem.* **2012**, *51*, 9395 – 9402.
[18] H. Zhang, H. Borrmann, N. Oeshler, C. Candolfi, W. Schnelle, M. Schmidt, U. Burkhardt, M. Baitinger, J. Zhao, Y. Grin, *Inorg. Chem.* **2011**, *50*, 1250 – 1257.
[19] J. D. Corbett, *Acc. Chem. Res.* **1981**, *14*, 239 – 246.
[20] U. Frank-Cordier, G. Cordier, H. Schaefer, *Z Naturforsch. B* **1982**, *37*, 119 – 126.
[21] a) S. C. Sevov, J. D. Corbett, *Inorg. Chem.* **1992**, *31*, 1895 – 1901; b) S. C. Sevov, J. D. Corbett, *J. Solid State Chem.* **1993**, *103*, 114 – 130.
[22] V. Elser, *Phys. Rev. B* **1985**, *32*, 4892 – 4898.
[23] A. I. Goldman, A. Kreyssig, S. Nandi, M. G. Kim, M. L. Caudle, P. C. Canfield, *Philos. Mag.* **2011**, *91*, 2427 – 2433.

